Field and Temperature Calculations in Transverse Flux Inductive Heating Devices heating non-paramagnetic Materials using Surface Impedance Formulations for non-linear Eddy-current Problems

W. Mai and G. Henneberger
RWTH Aachen, Institut für Elektrische Maschinen
Schinkelstraße 4, 52062 Aachen, Germany

***Abstract*—This paper presents the calculation of both the field and temperature distribution in thin moving non-paramagnetic sheets in transverse flux inductive heating devices (TFIH). The surface impedance formulation for non-linear materials is extended to this thin plate problem. The temperature distribution is obtained by solving Fourier's thermal conduction equation. In this non-linear coupled electromagneto-thermal problem the temperature dependencies of the B/H curve, the conductivity and the thermal conductivity are fully considered.**

***Index terms*—Induction heating, Finite element methods, Nonlinear estimation**

I. Introduction

In transverse flux heaters the magnetic field of symmetrically placed coils on both sides of a thin moving conducting sheet induces eddy-currents in it, which heat up the material continuously. Compared to longitudinal heaters a much lower frequency can be used resulting in a higher electrical efficiency, which is why transverse flux heaters are given priority in heating thin strips.

The numerical calculations of the TFIH using the finite element method in three dimensions face the problem that the sheet is of relatively small thickness compared to the size of the remaining parts, e.g. the coils and the air gap, which requires a large amount of elements.

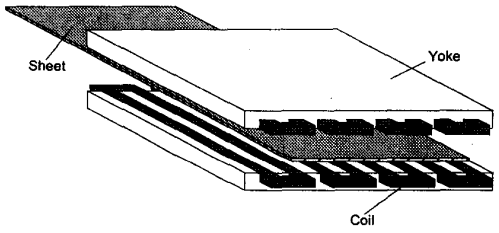

Fig. 1. The principle of the transverse flux heating

Several authors have presented the use of the surface impedance formulation for linear materials to reduce the size of the electro-magnetic problem [1]–[3]. This impedance replaces the 3d body of the conducting sheet by a 2d boundary condition and, therefore, reduces computational costs.

Methods for saturated non-paramagnetic materials are combined with the $T-\Omega$ method in [4] using the limit theory of [5], assuming the magnetic field on the surface is sinusoidal. Another formulation can be obtained if the electric field is assumed to be mostly sinusoidal [6].

The combination of both the linear and non-linear surface impedance has recently been used to calculate the losses in transformers [7], where the penetration depth δ_{nl} for non-linear materials is assumed to be smaller than the thickness of the replaced bodies, i.e. the tank wall.

In the TFIH device considered in this paper, δ_{nl} can be greater than the half-thickness of the conductor and the surface impedance formulation has to be modified. This paper extends the surface impedance for the case based on [5] and applies it to the problem. The method is compared to transient non-linear solutions of a test model using ANSYS showing the accuracy of the formulation.

The losses in the sheet are obtained using Poynting vectors. Fourier's thermal conduction equation leads to the temperature distribution using an upwind scheme. The temperature dependencies of the B/H curve, the conductivity and the thermal conductivity are fully considered.

II. The Surface Impedance Formulations

The surface impedance is defined as ratio of the tangential electric field E to the magnetic field H

$$\underline{Z}_s = \frac{\underline{E}_t}{\underline{H}_t} \tag{1}$$

with $\vec{\underline{H}}_{2t} = \vec{\underline{H}}_{1t}$ and $\vec{\underline{E}}_{2t} = \vec{\underline{E}}_{1t}$ shown in Fig. 2. Considering $\operatorname{curl} \vec{\underline{E}}_t = -j\omega \vec{\underline{B}}_n$ leads to

$$\operatorname{curl}(\underline{Z}_s(\vec{n} \times \vec{\underline{H}}_t)) = -j\omega\mu_0 \vec{\underline{H}}_n \tag{2}$$

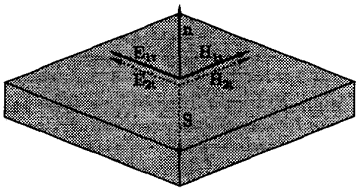

Fig. 2. The surface of the thin sheet

Manuscript received June 1, 1998.
G. Henneberger, e-mail henneberger@rwth-aachen.de;
W. Mai, e-mail mai@rwth-aachen.de.

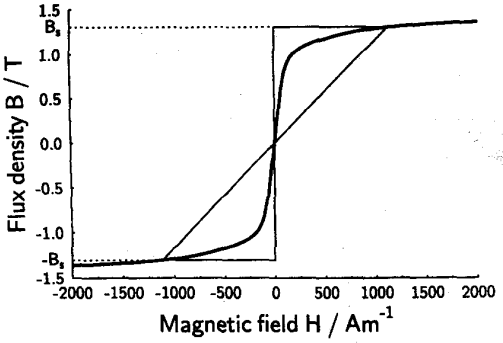

Fig. 3. Assumed non-linear B/H curve along with a linear and rectangular approximation

To solve the electromagnetic field problem of the TFIH device the $T-\Omega$ method is applied with

$$\operatorname{grad}\underline{\Omega} = \underline{\vec{H}} = \underline{\vec{H}}_n + \underline{\vec{H}}_t \ . \tag{3}$$

The term

$$\operatorname{curl}(\underline{\Omega}\vec{n}) = \underline{\Omega}\operatorname{curl}\vec{n} + \operatorname{grad}\underline{\Omega}\times\vec{n} = -\vec{n}\times\operatorname{grad}\underline{\Omega} \tag{4}$$

leads to the boundary condition for the scalar potential Ω replacing the body of the sheet[1]:

$$\operatorname{curl}(\underline{Z}_s(\operatorname{curl}(\underline{\Omega}\vec{n})) = j\omega\mu_0((\operatorname{grad}\underline{\Omega})\vec{n})\vec{n} \tag{5}$$

The losses w in the thin sheet are obained with the Poynting vector $\vec{S}$

$$\vec{S} = \vec{E}\times\vec{H} \tag{6}$$

$$\underline{S} = \frac{1}{2}\,\underline{E}_t\,\underline{H}_t^* = \frac{1}{2}\,\underline{Z}_s\,|\underline{H}_t|^2 = \frac{1}{2}\,\underline{Z}_s\,|\vec{n}\times\operatorname{grad}\underline{\Omega}|^2 \tag{7}$$

$$w = \frac{1}{2e}\mathrm{Re}\{\underline{Z}_s\}\,|\vec{n}\times\operatorname{grad}\underline{\Omega}|^2 \tag{8}$$

The surface impedance $\underline{Z}_s$ for non-linear materials, e.g. Fig. 3, is derived by combining the surface impedance for a linear and a rectangular approximation of the B/H curve.

A. Linear materials

In the case of linear materials the calculation of $\underline{Z}_s$ for thin sheets is known as

$$\underline{Z}_{sl} = \frac{1+j}{\delta_l\sigma}\frac{1}{\tanh\underline{\gamma}e} \tag{9}$$

where σ is the conductivity and $2e$ is the thickness of the sheet. With μ as the permeability and ω as the angular frequency, the penetration depth δ_l and $\underline{\gamma}$ are

$$\delta_l = \sqrt{\frac{2}{\omega\mu\sigma}} \quad \text{and} \quad \underline{\gamma} = j\omega\sigma\mu \ . \tag{10}$$

[1]using: $\vec{n}\times\operatorname{grad}\underline{\Omega} = \vec{n}\times\underline{\vec{H}}_n + \vec{n}\times\underline{\vec{H}}_t = \vec{n}\times\underline{\vec{H}}_t$ and $\vec{n}\operatorname{grad}\underline{\Omega} = \vec{n}\underline{\vec{H}}_n + \vec{n}\underline{\vec{H}}_t = \underline{H}_n$

B. Rectangular B/H curve

On the surface of the sheet the magnetic field $H_{sx}(t)$ and the electric field $E_{sy}(t)$ are related by the depth $\zeta(t)$ of a moving separating surface, where the eddy-currents are zero beyond [5]:

$$\frac{H_{sx}(t)}{\zeta(t)} = \sigma E_{sy}(t). \tag{11}$$

In transverse flux inductive heating devices the magnetic field is mostly perpendicular to the surface of the sheet because of the geometry and the high permeability.

The following discussion distinguishes between a penetration depth which is smaller than half of the sheet's thickness, and one which is larger.

If the penetration depth is *smaller* than half of the sheet's thickness then the electric field can be assumed to be mostly sinusoidal, leading to [6]:

$$2B_s\frac{d\zeta}{dt} = E_{sy}(t) = \hat{E}_s\sin\omega t \tag{12}$$

$$\Rightarrow \zeta(t) = \frac{\hat{E}_s}{2\omega B_s}(1-\cos\omega t) = \frac{\hat{E}_s}{\omega B_s}(\sin^2\frac{\omega t}{2}). \tag{13}$$

The maximum penetration depth follows:

$$\delta_{nl} = \frac{\hat{E}_s}{\omega B_s}. \tag{14}$$

Because (6) leads to $S(t) = E_{sy}(t)H_{sx}(t)$, only the fundamental component of $H_{sx}(t)$, namely $H_1(t)$, is of interest and can be obtained by Fourier analysis:

$$H_1(t) = \frac{\sigma\hat{E}_s^2}{2\omega B_s}\left(\sin\omega t - \frac{4}{3\pi}\cos\omega t\right). \tag{15}$$

The amplitude of $H_1(t)$ follows:

$$\hat{H}_1 = \frac{\sigma\hat{E}_s^2}{2\omega B_s}\sqrt{1+\frac{16}{9\pi^2}} \tag{16}$$

what leads finally to the boundary impedance:

$$\underline{Z}_{snl} = \sqrt{\frac{2\omega B_s}{\sigma\hat{H}_1}}\frac{1}{\sqrt[4]{1+\frac{16}{9\pi^2}}}e^{j23°} \tag{17}$$

and the penetration depth depending on $\hat{H}_1$:

$$\delta_{nl} = \sqrt{\frac{2\hat{H}_1}{\sigma\omega B_s}}\frac{1}{\sqrt[4]{1+\frac{16}{9\pi^2}}} \tag{18}$$

If the penetration depth is *larger* than half of the sheet's thickness, i.e. e, the two waves moving inward from the outside faces meet at the center before the end of the half-period leading to:

$$\zeta(t) = \begin{cases} \frac{\delta_{nl}}{2}(1-\cos\omega t) & : \ 0 < t < t_0 \\ e & : \ t_0 < t < \frac{T}{2} \end{cases} \ . \tag{19}$$

Where t_0 is the time when the separating surface reaches the middle of the plate $t_0 = \frac{1}{\omega}\arccos(1 - \frac{2e}{\delta_{nl}})$.

Further investigations revealed that $H_{sx}(t)$ follows almost the same curve as in the preceding passage

$$H_{sx}(t) = \frac{\hat{H}_1}{\sqrt{1+\frac{16}{9\pi^2}}} \sin\omega t(1-\cos\omega t). \qquad (20)$$

Using (11) and (19) the electrical field on the surface of the sheet is expressed as:

$$E_{sy}(t) = \begin{cases} \dfrac{2\hat{H}_1}{\delta_{nl}\sigma\sqrt{1+\frac{16}{9\pi^2}}} \sin\omega t & : 0 < t < t_0 \\ \dfrac{\hat{H}_1}{e\sigma\sqrt{1+\frac{16}{9\pi^2}}} \sin\omega t(1-\cos\omega t) & : t_0 < t < \dfrac{T}{2} \end{cases} \qquad (21)$$

Fig. 4 plots $E_{sy}(t)$ and $H_{sx}(t)$. The fundamental components are $\hat{E}_{1s}$ and $\hat{E}_{1c}$ with $K = \frac{2\hat{H}_1}{\sigma\sqrt{1+\frac{16}{9\pi^2}}}$ given by:

$$\begin{aligned} \hat{E}_{1s} &= \frac{4}{T}\int_0^{\frac{T}{2}} E_{sy}(t)\sin\omega t\, dt \\ &= \frac{4}{T}\frac{2\hat{H}_1}{\sigma\sqrt{1+\frac{16}{9\pi^2}}}\left[\frac{1}{\delta_{nl}}\int_0^{t_0}\sin^2\omega t\, dt + \frac{1}{2e}\int_{t_0}^{\frac{T}{2}}\sin^2\omega t(1-\cos\omega t)\, dt\right] \\ &= K\cdot \left[\frac{\omega t_0 - \sin\omega t_0\cos\omega t_0}{\delta_{nl}\pi} + \frac{3(\pi+\sin\omega t_0\cos\omega t_0-\omega t_0)+2\sin^3\omega t_0}{3d\pi}\right] \\ \hat{E}_{1c} &= \frac{4}{T}\int_0^{\frac{T}{2}} E_{sy}(t)\cos\omega t\, dt \\ &= \frac{4}{T}K\left[\frac{1}{\delta_{nl}}\int_0^{t_0}\sin\omega t\cos\omega t\, dt + \frac{1}{d}\int_{t_0}^{\frac{T}{2}}\sin\omega t\cos\omega t(1-\cos\omega t)\, dt\right] \\ &= K\left[\frac{\sin^2\omega t_0}{\delta_{nl}\pi} - \frac{5-3\cos^2\omega t_0+2\cos^3\omega t_0}{3d\pi}\right] \end{aligned} \qquad (22)$$

The absolute value and the angle of $\underline{Z}_{snl}$ are:

$$Z_{snl} = \frac{\sqrt{\hat{E}_{1s}^2+\hat{E}_{1c}^2}}{\hat{H}_1} \quad \text{and} \quad \varphi = 23° + \arctan\frac{\hat{E}_{1c}}{\hat{E}_{1s}} \qquad (23)$$

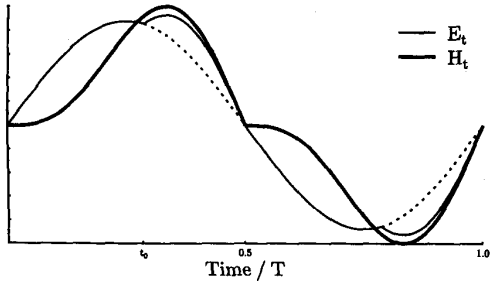

Fig. 4. The prediction of the electric and magnetic field on the surface for the rectangular B/H curve

To obtain the value for the surface impedance Z_{snl} the maximum penetration depth δ_{nl} has to be calculated first from (18). If δ_{nl} is smaller than the half-thickness of the sheet then Z_{snl} is calculated from (17). Otherwise, (23) is used.

C. Combining the linear and rectangular B/H curve

Equation (9) for the linear approximation and either (17) or (23) for the rectangular approximation of the B/H curve are combined in order to obtain the total surface impedance $\underline{Z}_s$ according to [7], [8] as

$$\underline{Z}_s = f(\hat{H}_1)\underline{Z}_{sl} + (1-f(\hat{H}_1))\underline{Z}_{snl}\ . \qquad (24)$$

The factor $f(\hat{H}_1)$ reflects the linearity of the B/H curve. In the case of a linear B/H curve $\underline{Z}_{sl}$ should be used, i.e. $f(\hat{H}_1) = 1$, whereas in the case of the rectangular curve $\underline{Z}_{snl}$ is the best approximation, i.e. $f(\hat{H}_1) = 0$. In order to cover the intermediate states this paper uses a smooth transition between both cases given as:

$$f(\hat{H}_1) = 2\left(1 - \frac{\int_0^{\hat{H}_1} B(h)\, dh}{B(\hat{H}_1)\hat{H}_1}\right) \qquad (25)$$

for every finite element.

III. Results

The proposed shape of the function of both the electric and magnetic field on the surface is verified with transient non-linear electromagnetic calculations using ANSYS, taking Fig. 3 into account. A two dimensional model represents a cross section of the TFIH device.

Fig. 5 shows the shape of both the electric and magnetic field at two positions of the surface. At position 1 the field does not reach the middle of the sheet, i.e. E_t is almost sinusoidal. At position 2 the field strength is larger than at position 1. Therefore, the depth of penetration is larger than the half-thickness and the fields follow the proposed curve of Fig. 4.

Fig. 6 shows the surface impedance Z_{sl} and Z_{snl} for the linear and rectangular approximation obtained from the transient ANSYS calculations for different field strengths. The comparison of the estimated total impedance Z_s (24) and the real value Z_{real} reveals a very good agreement.

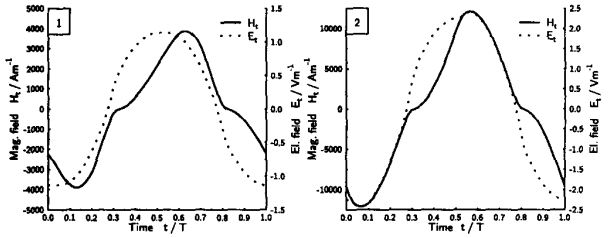

Fig. 5. Electric and magnetic field on the surface calculated with ANSYS for two field strengths

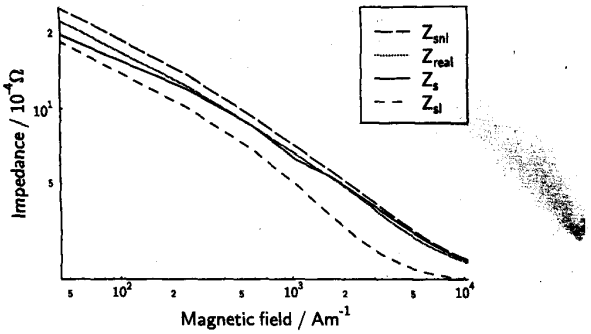

Fig. 6. Comparison of the surface impedance values

The boundary impedance formulations are included into the finite element formulations for the TFIH device. They describe the non-linear coupled problem, which consists of field and temperature calculations [9]. The flow of calculation is shown in Fig. 8. First the field problem is solved with the $T-\Omega$ method. The dependency of Z_s from Ω is considered in the first loop according to Fig. 8 and Fig. 7. Then the losses of the eddy-currents W are obtained. The temperature field is solved in a two dimensional mesh with respect to the temperature dependency

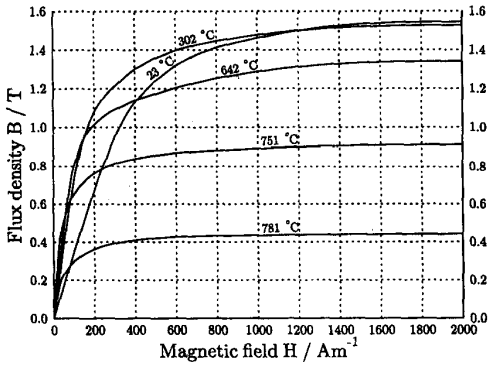

Fig. 7. The B/H curve as a function of the temperature

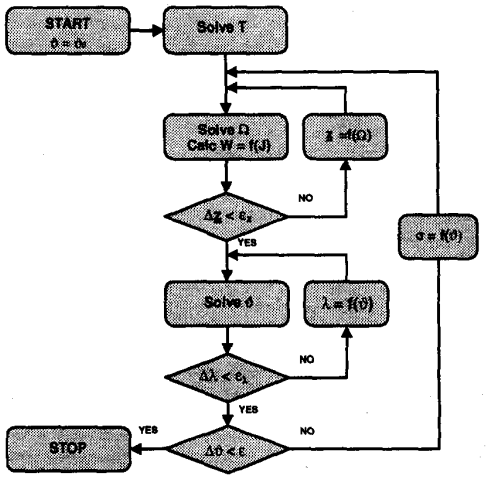

Fig. 8. The flow of calculation in this non-linear coupled problem

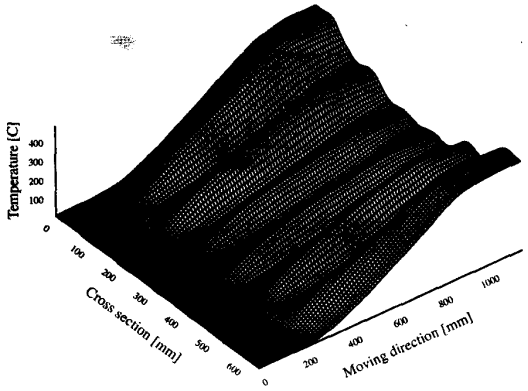

Fig. 9. The temperature distribution of the test TFIH device

of the thermal conductivity λ. The entire process is solved iteratively with respect to the temperature dependency of the conductivity σ. The resulting temperature distribution is shown for a test device in Fig. 9. It contains three parallel pairs of coils.

IV. Conclusions

This paper presents an extension of the surface impedance formulation for non-linear eddy-current problems and applies it to the temperature calculations of a transverse flux induction heating device. The numerical approximations of the surface impedance compared to transient field calculations reveal a good agreement.

References

[1] N. Allen, D. Rodger, H. C. Lai, P. J. Leonard, "Scalar-based finite element modelling of 3D eddy currents in thin moving conducting sheets", *IEEE Trans. Magn.*, vol. 32, no 3, pp. 733-736, May 1996.

[2] L. Krähenbühl, D. Muller, "Thin layers in electrical engineering. Example of shell models in analysing eddy-currents by boundary and finite element methods", *IEEE Trans. Magn.*, vol. 29, no 2, pp. 1450-1455, March 1993.

[3] J. Sakellaris, G. Meunier, X. Brunotte, C. Guérin, J. C. Sabonnadière, "Application of the impedance boundary condition in a finite element environment using the reduced potential formulation", *IEEE Trans. Magn.*, vol. 27, no 6, pp. 5022-5024, November 1991.

[4] T.W. Preston, A.B.J. Reece, "Solution of 3-dimensional eddy current problems: the T-Ω method", *IEEE Trans. Magn.*, vol. 18, no 2, pp. 486-491, March 1982.

[5] P.D. Agarwal, "Eddy-current losses in solid and laminated iron", *Trans. AIEE*, vol. 78, part I, pp. 169-181, 1959.

[6] D.A. Lowther, E.A. Wyatt "The computation of eddy current losses in solid iron under various surface conditions", *Compumag Conference*, Oxford, no 7, pp. 269-276, 1976.

[7] C. Guérin, G. Meunier, G. Tanneau, "Surface impedance for 3D non-linear eddy current problems -application to loss computation in transformers-", *IEEE Trans. Magn.*, vol. 32, no 3, pp. 808-811, May 1996.

[8] E.M. Deeley, "Flux penetration in two dimensions into saturating iron and the use of surface equations", *Proc. IEE*, vol. 126, no 2, pp. 204-208, February 1979.

[9] W. Mai, G. Henneberger, "Calculation of the Transient Temperature Distribution in a TFIH Device using the Impedance Boundary Condition", *IEEE Trans. Magn.*, Sep 1998, in press.